Structural-functional connectivity mapping of the insular cortex system: A combined data-driven and meta-analytic topic mapping approach

Benjamin Klugah-Brown[1#], Pan Wang[1#], Yuan Jiang[1], Benjamin Becker[1], Peng Hu[1], Bharat Biswal[1,2]*

[1]The Clinical Hospital of Chengdu Brain Science Institute, MOE Key Laboratory for Neuroinformation, Center for Information in Medicine, School of Life Science and Technology, University of Electronic Science and Technology of China, Chengdu, China; [2]Department of Biomedical Engineering, New Jersey Institute of Technology, Newark, NJ 07102, USA

[#]B.K-B. and P.W. contributed equally to this work.
*Bharat Biswal

Email: bbiswal@gmail.com

Author Contributions: B.K-B. and P.W. conceptualized, analyzed, and wrote the paper; Y.J. and P.H. analyzed DTI tracking, and B.B. and B.B. performed research.

Competing Interest Statement: The authors declare no competing interests**.**

Classification: Biological sciences.

Keywords: Diffusion tensor images, functional networks, insula, meta-analysis, resting-state functional connectivity

Abstract

The insular cortex is an important anatomical integration hub and can serve as a suitable model for exploring structural-functional relationships. In this study, we examined structural and functional magnetic resonance correspondence via the diffusion tensor imaging (DTI) and resting-state functional connectivity (RSFC) profiles of the insular cortex and its mapping with functional networks (FNs) across the brain. We explored these associations primarily by using a data-driven method to independently estimate the structural-functional connectivity in the human insular cortex system. Data were obtained from the Human Connectome Project comprising 108 resting-state functional magnetic resonance neuroimaging (fMRI) and DTI. Brain networks were acquired and defined according to the seven Yeo FNs. In general, we observed moderate to high association between the structural and functional mapping results of three distinct insular subregions: the posterior insula (sensorimotor: RSFC, DTI = 50%, 72%, respectively), dorsal anterior insula (ventral attention: RSFC, DTI = 83%, 83%, respectively), and ventral anterior insula (frontoparietal: RSFC, DTI = 42%, 89%, respectively). We also examined the cognitive and behavioral domains associated with these three insular subregions using meta-analytic topic mapping and found cognitive and behavioral relations to affective processes, reflecting the core properties of the cytoarchitecture. In sum, given the core role of the insula in the human brain, our findings on the correspondence of the insular cortex system between DTI and RSFC mappings provide a novel approach and insight for clinical researchers to detect dysfunctional brain organization in various neurological disorders.

Significance Statement

The insula is a suitable model for exploring the structural and functional relationships of the human brain. However, the correspondence between the connectivity profiles of the insula to FNs as derived from DTI and RSFC mapping is not adequately investigated. Here, we combined DTI and RSFC approaches to investigate the structural–functional correspondence of the insular cortex system. Our results revealed moderate to high overlap between the structural and functional mappings of the insular subregions, suggesting that a simple model of direct anatomical connectivity can elucidate the correlations in neuronal activity. The meta-analytic topic mapping approach further provided better inference for the cognitive and behavioral relations of the different insular subregions.

Introduction

The functional organization of the human brain modulates physical characteristics via a complementary association throughout its development and organization (1). Therefore, associating structural and functional connectivity is vital for understanding human brain functions and would significantly enrich our knowledge of neurobiological mechanisms underlying the brain. At cellular level, both invasive tracing and electrophysiology methods show brain functions that represent neural responses to an action potential. However, these approaches are limited methodologically and do not offer a means of examining the associations between the structures and functions across the whole brain. Accordingly, capitalizing on the development of functional magnetic neuroimaging (fMRI) and diffusion tensor imaging (DTI) (2) enables examination of the functional interactions and their structural underpinnings at the system level. Although dual imaging modalities have been combined for exploring the characteristics of the brain independently [see review in (3)], most studies focus on measuring brain activity in response to a specific task, where interpretations are often limited generally by few defined brain regions in the experiment, limiting the suitability for investigating the relationship across the whole brain. Therefore, to study the global characterization of the associations between the two modalities, a whole-brain organization-level approach would be appropriate for capturing the continual reshaping of the brain. Consequently, DTI and resting-state functional connectivity (RSFC) will prove to be a better alternative to the

activation-based approaches in previous studies (4–6). Motivated by recent studies (2, 7), the present study explored the correspondence between the structure and functional connections of human insular cortex mapping to functional network (FN) organization of the brain.

The insular cortex is an important anatomical integration hub with connections to the cortical and subcortical regions and can be a suitable model candidate for exploring the concordance between the structural and functional profiles. Besides, with respect to multimodality of the insula investigation, Kelly and colleagues explored the insular cortex using three independent imaging modalities: task-evoked coactivation, intrinsic functional connectivity, and gray matter covariance (4). They showed that the underlying brain organization consistently reflected the structural-functional tripartite cytoarchitecture of the insula. In the present study, we applied the concept of overlaps between two imaging modalities to the insular of healthy people obtained from resting-state and DTI data.

Moreover, with reference to the white matter tracts, several cortical and subcortical regions, including the frontal, parietal, hippocampus, and amygdala, were shown to be connected to the insula (8). Furthermore, using diffusion-weighted imaging, human studies have shown similar connectivity between the PI/AI and the anterior cingulate, frontal, parietal, and sensorimotor regions (9, 10). Independent studies involving structural tractography (11–13) and structural or functional connectivity analysis (14–16) have provided the basic capabilities of each imaging method for studying the insula in general.

Together, the above structural and functional connectivity studies of the insula provide an avenue for examining the core properties of the brain. However, these studies do not address the correspondence of the structural connectivity (DTI) and RSFC of the insular cortex and their mapping to FNs, thereby limiting overall understanding of the complementary association between the fiber tractography connectivity and resting-state imaging methods and how they may enhance clinical research in various mental disorders. Therefore, mapping the structural and functional connectivity overlaps of insular (subregions) to the larger networks of the whole brain would enable the description of well-defined characteristics underlying its varied functions across the brain.

In this work, we explored these associations using a data-driven method to first test the methodological consistency in the human insular cortex and its mapping to the FNs. We also used meta-analytic topic mapping to examine the cognitive and behavioral domains associated with each insular subregion obtained.

Results

Identification of Functional Insular Subregional Networks. Seven cortical FNs were defined based on Yeo's template: visual network (VSN), sensorimotor network (SMN), dorsal attention network (DAN), ventral attention network (VAN), limbic network (LIMB), frontoparietal network (FPN), and default mode network (DMN) (Fig. 1A). Fig. 1B depicts the distinct insular subregions with maximum voxels functionally connected to the FNs and computed through the winner-take-all algorithm. The algorithm takes into account one voxel within the insula per network. As a result, only six distinct insular subregions were connected to the six networks, leaving out the VSN (Fig. 1B, row 2, column 1). Based on the anatomical labeling of the insular subregions (11, 17), for low-order FN, we found that the SMN connected with the left/right/bilateral PI (left, dorsal granular; right, hypergranular; Fig. 1B, red). The DAN was also connected to the left PI (dorsal granular, Fig. 1B; blue). The subregion corresponding to the VAN and LIMB showed connectivity distribution in the bilateral dAI (dorsal granular and ventral dysgranular, Fig. 1B; yellow and cyan, respectively). Maximal connectivity with the FPN and DMN was mostly found in the left/right vAI (left; ventral granular, Fig. 1B, orange) and right vAI (ventral granular, Fig. 1B; green), respectively. Fig. 2A demonstrates the familywise error (FWE) computed on the voxels of each subregion; we observed distinctive patterns similar to the winner-take-all algorithm. The number of voxels (NOV) was distributed across the subregions. Maximal connectivity was observed in two insular subregions (vAI, left NOV = 6, right NOV = 26; vAI; left NOV = 206, right NOV = 222; vAI, left NOV = 33, right NOV = 21) connected to the VSN and FPN, respectively (Fig. 2A, column 1, 6, 7). Two dAI (region

1, left NOV = 990, right NOV = 968; region 2, left NOV = 207, right NOV = 148) were maximally connected to the VAN and LIMB, respectively (Fig. 2A, columns 4 and 5). For the PI, we found two subregions (region 1, left NOV = 419, right NOV = 496; region 2, left NOV = 48, right NOV = 48). SI Appendix, Table S1 shows the detailed peak coordinate of each insular subregion.

Structural Connectivity Between the FNs and Insular Subregions. For each participant, fiber bundles connecting each of Yeo's seven cortex networks and insular regions were estimated using TrackVis (www.trackvis.org). Through the 15% threshold of the participants' voxel allocation (2, 18), we identified significant mapping between the insular subregion and the FNs similar to the functional connectivity. Fig. 2B demonstrates the DTI connectivity of each subregion (column 1, left NOV = 254, right NOV = 198; column 6, left NOV = 1437, right NOV = 833; column 7, left NOV = 1686, right NOV = 832) categorized as vAI and connected to the VSN, FPN, and DMN, respectively. Also, the dAI subregions (column 4, left NOV = 3196, right NOV = 2339; column 5, left NOV = 733, right NOV = 319) were maximally connected to the VAN and LIMB, respectively (Fig. 2B). For PI, two subregions (column 2, left NOV = 1882, right NOV = 1542; column 3, left NOV = 237, right NOV = 97) demonstrated connectivity with the SMN and DAN (Fig. 2B). Details of the peak insula coordinates are shown in SI Appendix, Table S2.

Connectivity Overlap Between DTI and RSFC. The differences in the underlying physical characteristics of the two methods notwithstanding, there were significant ($P < 0.0001$) overlaps in the connectivity profile of each subregion mapping to each FN. Fig. 2C shows the overlap between the RSFC and DTI results (SI Appendix, Table S3). The insula connectivity demonstrated a similar pattern mapping to the FNs. The DTI and RSFC significantly overlapped largely with all regions and mapped to all FNs except the VSN. The overlap of the insular subregion corresponding to the DAN between the DTI and RSFC was exceptionally low (<7%, $P = 0002$) for both the winner-take-all algorithm and the FWE computation. Based on the following criteria: low (0–0.19), low–moderate (0.2–0.39), moderate (0.4–0.59), moderate-high (0.6–0.79), or high (0.8–1) as defined in (2), three significant insular regions showed greater than moderate overlap (Fig. 2C, column 2, 4, 6, SI Appendix, Table S3), suggesting the largest overlap between DTI and RSFC (PI-SMN [PI related to the SMN], RSFC = 50%, DTI = 72%; dAI-VAN [dAI associated with the VAN], RSFC = 83%, DTI = 83%; vAI-FPN [vAI associated with the FPN], RSFC = 42%, DTI = 89%). Based on the percentage overlaps in SI Appendix, Table S3, we recomputed the winner-take-all algorithm and the FWE for the three distinct insular subregions, namely the PI (Brodmann area 22), dAI (Brodmann area 44), and vAI (Brodmann area 4) (Fig. 3A, B, C); the cytoarchitecture of the three regions (Fig. 3D) resembled previously reported cluster analysis results (19).

Topic Mapping the Insular Subregions. We examined the relationships between the insular subregions (left and right) and the various cognitive and behavioral terms. Fig. 4 shows that both the uniformity test and associative test were significantly related with various terms in the database, such as pain: "Pain painful chronic" was most prevalent amongst all the three subregions; decision: "decision-making choice"; empathy: "empathy social empathy"; and inhibition control such as "Stroop interference control" were significantly related to the dAI and vAI. The PI was typically correlated to motor-related topics: "motor cortex sensorimotor", while the dAI was particularly related to social cognition: "social cognition control". Executive control, social trust, and auditory were significantly related to "executive control cognition", "game social trust" and "hallucination auditory", respectively. The PI and vAI were both significantly associated with taste-related topics: "taste swallow gustatory". On the other hand, the associative test showed a more detailed relationship, with executive control and sensorimotor significantly associated with the left vAI and PI, respectively, whereas inhibition control was related to the right dAI and vAI. SI Appendix, Table S5 shows the detailed loaded topics and number of studies contributing to the terms.

Discussion

In the present study, we demonstrated the correspondence between the structural and functional connectivity of the insular (subregions) and their mapping to FNs. This approach highlights the basic structural-functional connectivity relationship of the tripartite architecture of the insula, with subregional distribution comprising the PI, dAI, and vAI. The generally moderate to high structural-functional correspondence revealed through the overlaps validated the potential mapping of insular subcortical connectivity via the two independent imaging methods and reflects the complementary relationship between the DTI and RSFC. Pairing the RSFC to the DTI tracts showed that the three distinctive insular regions were mapped significantly to three of the seven FNs including SMN, VAN, and FPN, and indicating a direct physical connection. Notably, these regions are consistent with the cytoarchitecture of the insular cortex identified in earlier studies (1, 20–23) and linked to large-scale FNs (22, 24). Moreover, the meta-analytic topic mapping, performed in a relatively large database composed of topics and terms, provides an additional perspective of the different insular subregions and how they are associated with various cognitive and behavioral domains across the networks.

Insular Connectivity Mapping to FNs. The functional and structural correspondence of the insular subregions is imperative for understanding the diverse functions and relations it has with whole-brain networks. There is a wide array of both structural (25, 26) and functional (11, 27) profiles, providing insight into the connectivity of the distinct regions shown in the present study. The insular subregions are consistent with that in previous functional (28) and meta-analytical (23) studies. Regarding the correspondence of the two imaging methods contributing to the connectivity of brain networks, Zhang and colleagues examined the differences and overlap between the structural and functional connectivity of the thalamus corresponding to cortical areas of the brain (29) and suggested a potential intersection of the thalamic system linking to specific cortical and subcortical regions across the brain. Jiang et al. showed a cortical connectivity profile that offset the dysfunctions associated with the motor perception networks of the gray matter in patients with schizophrenia (30). In agreement with the abovementioned studies, our study demonstrates DTI intersecting with RSFC, suggesting a compensatory relationship between each method.

Accordingly, in the present study, we observed three distinct structural and functional regions with significant overlapping and significantly mapped specific FNs. Based on the structural and functional correspondence, we found different levels of percentage connectivity of overlap. For example, the VSN, DAN, and LIMB were highly significant ($P < 0.0001$) but showed lower overlap; in contrast, the SMN, VAN, and FPN showed significant overlap for both RSFC and DTI mapping (SI Appendix, Table S3). We posit that the observed correlations of the RSFC and DTI fiber connection to the FNs was due to the unique insular subregions mapping to the FNs and reflect its significant role in cognitive functions. The greatest overlap using percentage voxel count was exhibited in mapping with the VAN (Fig. 2C, column 4, SI Appendix, Table S3); the extent of the overlap suggested a strong compensatory mechanism between the functional and structural connectivity with uniform correlation among the FNs and indicating that both methods contribute to global characterization at system level.

Moreover, the overall percentage overlaps reflect their significant role in connectivity between the insular subregions through the FNs. Another vital point revealed was that both the winner-take-all algorithm and the FWE demonstrated high structural connectivity mapping with the FNs as compared to the RSFC, with the highest overlap occurring in the dAI mapping to the VAN. The variability in the level of correspondence between the two imaging methods was due to DTI connectivity being fairly consistent over time (29). The DTI represents physical connection, with significant stability relative to functional connectivity, which in contrast represents synaptic neuronal activity, and exhibiting more variability over time (31). Additionally, the two imaging methods were expected to be different due to their underlying characteristics, interestingly, significant overlaps were found with a stricter threshold ($P < 0.0001$), suggesting that DTI and RSFC have compensated each other in the overall connectivities.

Insular Subregional mapping to FNs. Remarkably, the parcellation through the winner-take-all algorithm and the FWE was distributed within the borders of the insular cortex. The distinct

subregions were initially grouped in two major subregions: the AI and the PI (Fig. 1B, SI Appendix, Table S1). The overlap scores further grouped the region into three distinct subregions: PI, dAI, and vAI (Fig. 3A–C, D, SI Appendix, Table S4), consistent with that reported previously (19, 23). Kurth and colleagues reported four functional divisions of the insula: PI (involved in sensorimotor processes), central part (involved in olfactory and gustatory processes), and the vAI–dAI (involved in cognitive and socioemotional processes) (22); the functional distribution echoed that in the present study, with the central part further reorganized to the dAI (Fig. 3B).

The functional and structural PI mapped significantly to the SMN (Fig. 1A, B; column 2), with regional connectivity including primary/secondary motor and somatosensory similar to those reported in previous insula parcellation studies (4, 19). Interestingly, the observed structural-functional overlap reflected the widespread physical and neural complements implicated in the SMN. Prior functional studies using a data-driven approach reported that the regions found in the network showed precentral, postcentral, and sensorimotor areas (32), similarly in connectivity studies involving somatosensory and interoceptive processes (33–37). Combined, the abovementioned studies and our findings reflected the contribution to the primary regions involved in affective and somatosensory processes.

From the anterior side of the insula, there were two further divisions: dAI and vAI, occupying the central and anterior sections of the insular cortex (Fig. 3B, C), respectively. The dAI (Fig. 3B) mapped to the VAN (Fig. 1A4), with high connectivity in the frontal, anterior cingulate, and parietal areas functionally consistent with the clustering method (19). The VAN is implicated in attentional and awareness stimuli (38, 39) during tasks. The structural-functional overlap (83% overlap, Fig. 2C; columns 2 and 4, SI Appendix, Table S3) demonstrated the consistency of the physical connectivity most relevant to the dAI. In addition, the dAI is functionally related to the brain areas involved in cognitive control processes (40). In their clustering analysis, Deen et al. reported significant connectivity between the dAI and the regions involved in attention controls (19), which is in agreement with our results involving the VAN.

Ventrally in the AI, the results demonstrated significant vAI (Fig. 3C) mapping to the FPN (Fig. 1A, column 6), with significant overlap between DTI and RSFC, which includes the anterior cingulate cortex (ACC), posterior parietal cortex, and mid/superior frontal cortex. Unlike the dAI, the vAI exhibited a relative imbalance overlap, in which the maximum percentage was demonstrated in the DTI profile (SI Appendix, Table S3); this may suggest the extent of the voxels from the neighboring dAI. Functionally, the FPN comprised mainly the ACC, frontal, and parts of the parietal regions. The significant correspondence between the structural-functional vAI mapping to the FPN suggests the role of salience detection cognitive control (41).

Additionally, Medford and Critchley reviewed the functional relationship between the AI and the ACC and highlighted the complementary relationships, representing sensory input and awareness processes (42). The posterior part of the ACC has also been suggested to strongly correlate with the vAI and exhibits salience characteristics (41, 43, 44). Further, for emotions, pain from nociception is a vital sensory perception associated with both the vAI and dAI; the vAI is also associated with neuropathic pain (45). Although structural evidence through DTI is limited, its high overlap with RSFC suggested an important mapping between the vAI and the FPN.

Meta-Analytic Topic Mapping. The three subregions identified are consistent with previous studies (11, 23) and reflect the functional mapping between the subregions and the three FNs. The combined approach using topic mapping enabled further characterization of the various brain states to specific or overlapped subregions. This was achieved using the uniformity (formally known as forwarding inference) and associative (formally known as reverse inference) tests, which showed different cognitive/behavioral domains associated with each region. Consequently, both the uniformity and associative tests demonstrated a consistent association with “pain” in all three regions (SI Appendix, Fig. 4, Table S5). In accordance with previous studies, the attribution of the somatosensory response to the insula was generally pronounced throughout the various topics in the database. In particular, although specialized pain sensations have been identified for the whole of the insula region, the PI is mostly associated with thermosensory response (46, 47).

Interestingly, in the associative test, we observed specificities of the activations for the terms unique to the subregions. For example, while the uniformity test showed “inhibition control” exhibited in both the left and right dAI and vAI, the associative test further showed associations with the left dAI/vAI (Fig. 4). Moreover, both the dAI and vAI are strongly linked to topics involving emotion, empathy, and higher cognition, including social trust such as gaming, with dAI having a greater emphasis on goal-directed tasks, supporting characteristics of the VAN (28).

By combining both RSFC and DTI and examining their overlaps, we demonstrate a potential approach for investigating whole-brain progression. More importantly, the combined methods enabled the estimation of the relationships between the functional and anatomical connectivity that best describe the insula. Interestingly, the results echoed that of both functional (19) and structural (11) independent studies. Our study also reflects the importance of the relationship between the two methods. In addition, using meta-analysis to expand and characterize the insular subregions in behavioral and cognitive domains across specific FNs provided a comprehensible view of the advantage of this work, which can be replicated with any data.

Limitations

Although the present work represents a comprehensive approach for examining the intersection of RSFC and DTI profiles of the insula, some limitations should be considered. First, issues with model crossing fiber in DTI were inadequately represented, especially within the cerebral cortex, such as in the centrum semiovale (48); this is a potential problem in Human Connectome Project (HCP) data that could be solved using high-quality imaging, which would enhance fiber tracking in the white matter (49). Second, the image registration stages could have generated a potential error, as this step involves registering the images to different spaces.

Conclusion

Our study combines a data-driven approach and meta-analytic topic mapping and demonstrates the correspondence between the structural and functional connectivity of insular subregions mapped to FNs. Our findings reinforce the tripartite subregions of the insula including the PI, dAI, and vAI, which were significantly mapped to the SMN, VAN, and FPN, respectively. Generally, the significant connection between the DTI and RSFC results is profound and strengthens the idea that mapping between DTI and RSFC may provide a complementary association in each of these different measures. Furthermore, the additional application of the large-scale meta-analysis provided an unbiased approach for verifying the subregions and how the anatomical spatial arrangement can be based on functional connectivity with its associated affective/chemosensory and sensorimotor processing across the networks.

Materials and Methods

Data Acquisition. We obtained 119 healthy participants from the HCP dataset, of which 108 (11 DTI participants’ datasets were of different parameters) were used for the entire analysis, similar to our previous study (2). Although the dataset included resting-state fMRI with four runs (rfMRI_rest1_LR, rfMRI_rest1_RL, rfMRI_rest2_LR, rfMRI_rest2_RL), for T1-weighted images, we used a single run (rfMRI_rest1_LR) similar to the abovementioned previous study. See SI Materials and Methods for acquisition details.

Functional and DTI Data Preprocessing. The functional images were preprocessed using a combination of toolboxes: Data Processing Assistant for Resting-State fMRI (http://rfmri.org/DPARSF) and SPM12 (http://www.fil.ion.ucl.ac.uk/spm/software/spm12). The DTI preprocessing involved: normalization of b0 image intensity with the following correction; EPI

distortions, eddy current distortions, participant movements, and gradient nonlinearities (50). All preprocessing steps were similar to our previous work (2). See SI Materials and Methods for acquisition details.

Identification of Insula Functional Subregional Networks. We obtained seven functional cortical networks from Yeo's template (24) (downloaded from https://surfer.nmr.mgh.harvard.edu/fswiki/CorticalParcellation_Yeo2011): VSN, SMN, DAN, VAN, LIMB, FPN, and DMN. The insula mask was obtained from Harvard-Oxford cortical and subcortical structural atlases (https://neurovault.org/collections/262/). We excluded the insula voxels within the Yeo networks. Then, for each participant, the partial correlation was computed between every voxel time series within the insula mask, and we averaged the time series of each cortex network while controlling the impact of the temporal contributions from the remaining six cortex networks. Fisher's Z transform was performed on all correlation coefficients. To obtain the associated subregions, we projected the correlation coefficient to each voxel corresponding to the insula. A statistical *t*-map of connectivity pattern was obtained by calculating a one-sample *t*-test across all participants. To finally obtain the insular subregions corresponding to each FN subregion (seven FNs), we used the winner-take-all algorithm by selecting the most similar profile of connectivity for each insular voxel. As the winner-take-all method assumes that one voxel within the insula only corresponds to a single network, we performed a statistical correction of the one-sample *t*-test map of each cortex network as a region of interest (ROI) ($P < 0.05$, familywise error [FWE]-corrected) to obtain a more comprehensive understanding of the relation between the insula and FNs.

Identification of Insula Structural Subregional Networks. We selected the seven Yeo FNs and insula mask as ROIs for the DTI images. Before tracking the fibers connecting the FNs and insula, these FNs and insula mask were resampled to standard MNI diffusion space with a voxel size of $1.25 \times 1.25 \times 1.25$ mm^3. For each participant, we extracted the fiber bundles from the whole-brain fibers connecting each FN and insula, which was implemented in TrackVis. Subsequently, we accumulated these fiber bundles corresponding to each FN across all participants to establish a population-based probabilistic map of commissural tracts using the approach of Park et al. (51). The computations resulted in population probabilistic maps whose connectivity value corresponded to the number of samples with a trajectory from the insula mask through voxels and then to the cortical target mask. Essentially, a voxel was identified as part of a tract if it belonged to at least 15% (52, 53) of the participants. The procedure was aimed at validating the harmony between the anatomical properties and the functional connectivity.

Examining the Significant Overlap Between DTI and RSFC Mappings. Using the Monte Carlo method (31), we examined the significant overlap of insular subregions between the DTI and RSFC mapping. To ascertain these overlaps, we used all insular voxels and assigned each insular voxel a binary value (0 and 1). We then determined the proportion of voxels with a value of 1 by computing a 15% threshold of the total NOV in the DTI and RSFC (statistically significant threshold at $P < 0.05$, FWE-corrected). Overlap between the DTI and RSFC mapping was defined as the number of simulated voxels containing a value of 1 in both maps. A random permutation was performed 10,000 times, which assigned a value of 1 to the DTI and RSFC voxels. A statistical significance level was calculated by estimating the null distribution and NOV in the overlap. We categorized the overlaps using the following criteria: low (0–0.19), low–moderate (0.2–0.39), moderate (0.4–0.59), moderate-high (0.6–0.79), or high (0.8–1) as defined in (2).

Meta-Analytic Topic Mapping. We were interested in the overlaps between a set of terms associated with each insular division and existing topics in the Neurosynth database. For each term, we obtained two different statistical inference maps: the uniformity test map and the association test map (false discovery rate [FDR]-corrected (q) = 0.01). The uniformity map indicates the extent to which each brain voxel is consistently activated in studies for a specific term. The association test map indicates whether the activity in a voxel occurs more specifically for studies using the term of interest than for studies not using this term.

Acknowledgments

This work was supported by the National Key Research and Development Program of China (Grant No. 2018YFA0701400), National Natural Science Foundation of China (NSFC, No. 91632117), and the Science, Innovation and Technology Department of Sichuan Province (No. 2018JY0001).

References

1. L. Q. Uddin, J. S. Nomi, B. Hébert-Seropian, J. Ghaziri, O. Boucher, Structure and Function of the Human Insula. *J. Clin. Neurophysiol.* **34** (2017).

2. P. Wang, *et al.*, Structural and functional connectivity mapping of the human corpus callosum organization with white-matter functional networks. *Neuroimage* **227** (2021).

3. E. Rykhlevskaia, G. Gratton, M. Fabiani, Combining structural and functional neuroimaging data for studying brain connectivity: A review. *Psychophysiology* **45** (2008).

4. C. Kelly, *et al.*, A convergent functional architecture of the insula emerges across imaging modalities. *Neuroimage* **61** (2012).

5. A. A. Baird, M. K. Colvin, J. D. VanHorn, S. Inati, M. S. Gazzaniga, Functional connectivity: Integrating behavioral, diffusion tensor imaging, and functional magnetic resonance imaging data sets. *J. Cogn. Neurosci.* **17** (2005).

6. A. T. Toosy, *et al.*, Characterizing function-structure relationships in the human visual system with functional MRI and diffusion tensor imaging. *Neuroimage* **21** (2004).

7. Z. Long, *et al.*, Thalamocortical dysconnectivity in paroxysmal kinesigenic dyskinesia: Combining functional magnetic resonance imaging and diffusion tensor imaging. *Mov. Disord.* **32** (2017).

8. M. J. C. Showers, E. W. Lauer, Somatovisceral motor patterns in the insula. *J. Comp. Neurol.* **117** (1961).

9. L. L. Cloutman, R. J. Binney, M. Drakesmith, G. J. M. Parker, M. A. Lambon Ralph, The variation of function across the human insula mirrors its patterns of structural connectivity: Evidence from in vivo probabilistic tractography. *Neuroimage* **59** (2012).

10. J. Ghaziri, *et al.*, The Corticocortical Structural Connectivity of the Human Insula. *Cereb. Cortex* **27** (2017).

11. J. S. Nomi, E. Schettini, I. Broce, A. S. Dick, L. Q. Uddin, Structural connections of functionally defined human insular subdivisions. *Cereb. Cortex* **28** (2018).

12. L. Nanetti, L. Cerliani, V. Gazzola, R. Renken, C. Keysers, Group analyses of connectivity-based cortical parcellation using repeated k-means clustering. *Neuroimage* **47** (2009).

13. P. Hagmann, *et al.*, White matter maturation reshapes structural connectivity in the late developing human brain. *Proc. Natl. Acad. Sci. U. S. A.* **107** (2010).

14. J. Ghaziri, *et al.*, Subcortical structural connectivity of insular subregions. *Sci. Rep.* **8** (2018).

15. F. Cauda, *et al.*, Functional connectivity of the insula in the resting brain. *Neuroimage* **55**

(2011).

16. C. J. Honey, *et al.*, Predicting human resting-state functional connectivity from structural connectivity. *Proc. Natl. Acad. Sci. U. S. A.* **106** (2009).

17. J. Stelzer, E. Lacosse, J. Bause, K. Scheffler, G. Lohmann, Brainglance: Visualizing Group Level MRI Data at One Glance. *Front. Neurosci.* **13** (2019).

18. D. B. Archer, S. A. Coombes, N. R. McFarland, S. T. DeKosky, D. E. Vaillancourt, Development of a transcallosal tractography template and its application to dementia. *Neuroimage* **200** (2019).

19. B. Deen, N. B. Pitskel, K. A. Pelphrey, Three systems of insular functional connectivity identified with cluster analysis. *Cereb. Cortex* **21** (2011).

20. M. -Marsel Mesulam, E. J. Mufson, Insula of the old world monkey. Architectonics in the insulo-orbito-temporal component of the paralimbic brain. *J. Comp. Neurol.* **212** (1982).

21. J. R. Augustine, Circuitry and functional aspects of the insular lobe in primates including humans. *Brain Res. Rev.* **22** (1996).

22. F. Kurth, K. Zilles, P. T. Fox, A. R. Laird, S. B. Eickhoff, A link between the systems: functional differentiation and integration within the human insula revealed by meta-analysis. *Brain Struct. Funct.* **214** (2010).

23. L. J. Chang, T. Yarkoni, M. W. Khaw, A. G. Sanfey, Decoding the role of the insula in human cognition: Functional parcellation and large-scale reverse inference. *Cereb. Cortex* **23** (2013).

24. B. T. T. Yeo, *et al.*, The organization of the human cerebral cortex estimated by intrinsic functional connectivity. *J. Neurophysiol.* **106**, 1125–1165 (2011).

25. R. D. Shura, R. A. Hurley, K. H. Taber, Insular cortex: Structural and functional neuroanatomy. *J. Neuropsychiatry Clin. Neurosci.* **26** (2014).

26. V. Menon, *et al.*, Microstructural organization of human insula is linked to its macrofunctional circuitry and predicts cognitive control. *Elife* **9** (2020).

27. A. Jezzini, F. Caruana, I. Stoianov, V. Gallese, G. Rizzolatti, Functional organization of the insula and inner perisylvian regions. *Proc. Natl. Acad. Sci. U. S. A.* **109** (2012).

28. S. M. Nelson, *et al.*, Role of the anterior insula in task-level control and focal attention. *Brain Struct. Funct.* **214** (2010).

29. Z. Zhang, *et al.*, Altered functional-structural coupling of large-scale brain networks in idiopathic generalized epilepsy. *Brain* **134** (2011).

30. Y. Jiang, *et al.*, White-matter functional networks changes in patients with schizophrenia. *Neuroimage* **190** (2019).

31. D. Zhang, A. Z. Snyder, J. S. Shimony, M. D. Fox, M. E. Raichle, Noninvasive functional and structural connectivity mapping of the human thalamocortical system. *Cereb. Cortex* **20** (2010).

32. C. F. Beckmann, M. DeLuca, J. T. Devlin, S. M. Smith, Investigations into resting-state connectivity using independent component analysis. *Philos. Trans. R. Soc. B Biol. Sci.* **360**,

1001–1013 (2005).

33. X. Wang, *et al.*, Anterior insular cortex plays a critical role in interoceptive attention. *Elife* **8** (2019).

34. E. Kuehn, K. Mueller, G. Lohmann, S. Schuetz-Bosbach, Interoceptive awareness changes the posterior insula functional connectivity profile. *Brain Struct. Funct.* **221** (2016).

35. A. D. Craig, How do you feel? Interoception: The sense of the physiological condition of the body. *Nat. Rev. Neurosci.* (2002) https:/doi.org/10.1038/nrn894.

36. F. McGlone, *et al.*, Functional neuroimaging studies of human somatosensory cortex in *Behavioural Brain Research*, (2002).

37. H. Olausson, *et al.*, Unmyelinated tactile afferents signal touch and project to insular cortex. *Nat. Neurosci.* **5** (2002).

38. I. Indovina, E. MacAluso, Dissociation of stimulus relevance and saliency factors during shifts of visuospatial attention. *Cereb. Cortex* **17** (2007).

39. J. T. Serences, *et al.*, Coordination of voluntary and stimulus-driven attentional control in human cortex. *Psychol. Sci.* **16** (2005).

40. N. U. F. Dosenbach, *et al.*, Distinct brain networks for adaptive and stable task control in humans. *Proc. Natl. Acad. Sci. U. S. A.* **104** (2007).

41. W. W. Seeley, *et al.*, Dissociable intrinsic connectivity networks for salience processing and executive control. *J. Neurosci.* **27** (2007).

42. N. Medford, H. D. Critchley, Conjoint activity of anterior insular and anterior cingulate cortex: awareness and response. *Brain Struct. Funct.* **214** (2010).

43. S. Marek, N. U. F. Dosenbach, The frontoparietal network: Function, electrophysiology, and importance of individual precision mapping. *Dialogues Clin. Neurosci.* **20** (2018).

44. D. S. Margulies, *et al.*, Mapping the functional connectivity of anterior cingulate cortex. *Neuroimage* **37** (2007).

45. S. Ferraro, *et al.*, Dysregulated anterior insula reactivity as robust functional biomarker for chronic pain – convergent evidence from neuroimaging meta-analysis Dysregulated anterior insula reactivity as robust functional biomarker for chronic pain – convergent evidence fro. *medRxiv* (2021).

46. B. Baier, *et al.*, Insula and sensory insular cortex and somatosensory control in patients with insular stroke. *Eur. J. Pain (United Kingdom)* **18** (2014).

47. A. D. Craig, K. Chen, D. Bandy, E. M. Reiman, Thermosensory activation of insular cortex. *Nat. Neurosci.* **3** (2000).

48. V. J. Wedeen, *et al.*, Diffusion spectrum magnetic resonance imaging (DSI) tractography of crossing fibers. *Neuroimage* **41** (2008).

49. K. H. Maier-Hein, *et al.*, Author Correction: The challenge of mapping the human connectome based on diffusion tractography. *Nat. Commun.* **10** (2019).

50. M. F. Glasser, *et al.*, The minimal preprocessing pipelines for the Human Connectome

Project. *Neuroimage* **80** (2013).

51. H. J. Park, *et al.*, Corpus callosal connection mapping using cortical gray matter panellation and DT-MRI. *Hum. Brain Mapp.* **29** (2008).

52. S. Khalsa, S. D. Mayhew, M. Chechlacz, M. Bagary, A. P. Bagshaw, The structural and functional connectivity of the posterior cingulate cortex: Comparison between deterministic and probabilistic tractography for the investigation of structure-function relationships. *Neuroimage* **102** (2014).

53. I. J. Bennett, D. J. Madden, C. J. Vaidya, J. H. Howard, D. V. Howard, White matter integrity correlates of implicit sequence learning in healthy aging. *Neurobiol. Aging* **32** (2011).

Figures and Tables

Figure 1.

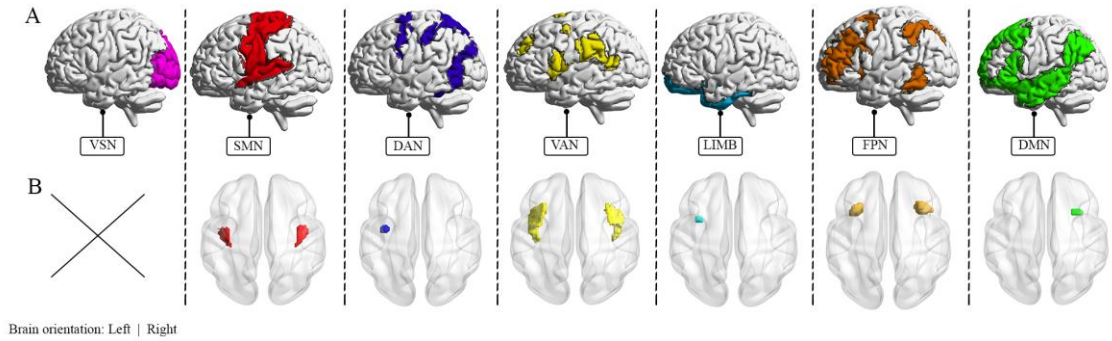

Winner-take-all projections of the subregional insula maps. (*A*) The cortex is partitioned based on major anatomical landmarks into seven nonoverlapping FNs as defined in (24). (*B*) Each insular subregional voxel is labeled with the color of the FN that produced the highest partial correlation values using RSFC. The empty cell indicates no voxel per the criterion of the winner-take-all algorithm; the subregion had too few voxels to survive the iteration.

Figure 2.

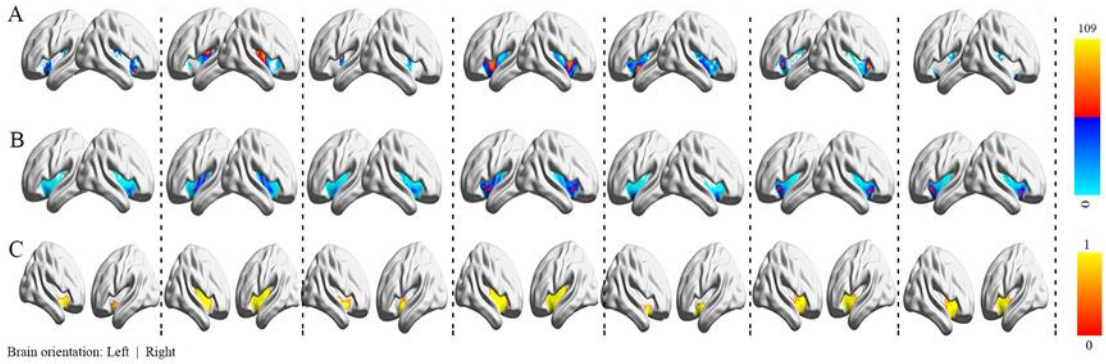

Functional and structural connectivity of insular cortex. (*A*) Functional connectivity profile; each FN in Figure 1A shows specific correlations in its neuronal activity with distinct insular subregions. The results were thresholded using FWE following the winner-take-all algorithm shown in Figure 1B. (*B*) Structural connectivity derived from probabilistic tractography demonstrated specificity of tracking white matter fiber tracts between the insula and each FN; all structural results were obtained after thresholding to 15% of the total participant voxels. (*C*) Structural and functional mapping demonstrated significant overlap in their connectivity profiles (yellow).

Figure 3.

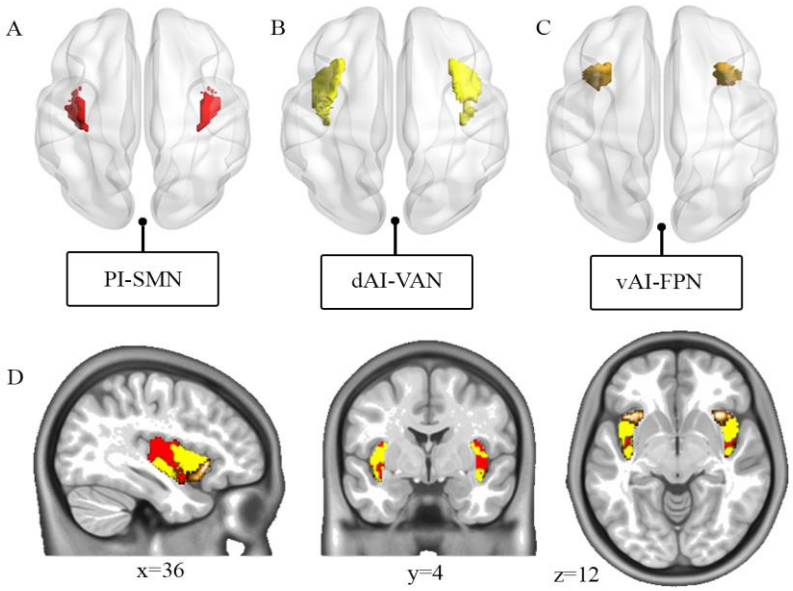

Final insular subregions. (*A*–*C*) Winner-take-all computed for three distinctive insular subregions; each color signifies a specific voxel. Each voxel was mapped to the FNs as follows: PI-SMN, dAI-VAN, and vAI-FPN. (*D*) FWE results are similar to the winner-take-all results displayed in the orthogonal view.

Figure 4.

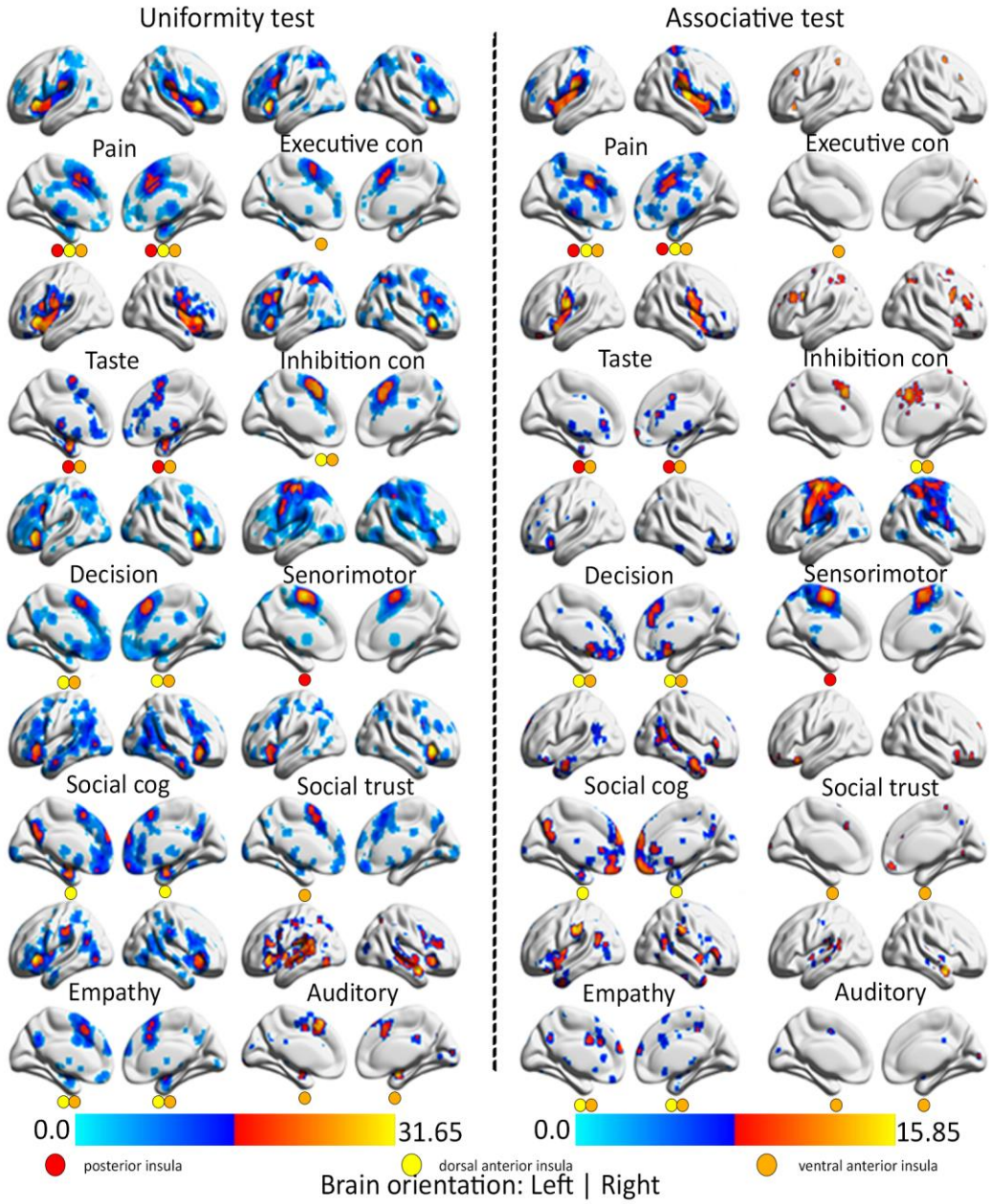

Meta-analytic topic mapping. The uniformity test and associative test were performed with various topics in the Neurosynth database. Each term signifies cognitive and behavioral domains of studies in the database. Social cog; social cognition, inhibition con; inhibition control; circles denote topics associated with each insular subregion. Significant area threshold at $P < 0.01$.